Assessing ultrasonic and optical flow velocimetry in a millifluidic device using oil-in-water emulsions as blood mimicking fluid

Lu, Estelle; Flores Cisternas, Williams; Uhl, Héloïse; Chargueraud, Alexandre; Grimal, Quentin; Renaud, Guillaume; Minonzio, Jean Gabriel; Fattaccioli, Jacques

DOI
10.1016/j.mne.2025.100298

Publication date
2025

Document Version
Final published version

Published in
Micro and Nano Engineering

MNE 27 (2025) 100298

Contents lists available at ScienceDirect

Micro and Nano Engineering

journal homepage: www.sciencedirect.com/journal/micro-and-nano-engineering

Assessing ultrasonic and optical flow velocimetry in a millifluidic device using oil-in-water emulsions as blood mimicking fluid

Estelle Lu [a,b], Williams Flores Cisternas [c], Héloïse Uhl [a,b], Alexandre Chargueraud [a,b], Quentin Grimal [d], Guillaume Renaud [e], Jean-Gabriel Minonzio [c,*], Jacques Fattaccioli [a,b,*]

[a] CPCV, Département de Chimie, École Normale Supérieure, PSL University, Sorbonne Université, CNRS, 75005 Paris, France
[b] Institut Pierre-Gilles de Gennes pour la Microfluidique, 75005 Paris, France
[c] Escuela de Ingeniería Informática, Center of Interdisciplinary Biomedical and Engineering Research for Health - MEDING, Universidad de Valparaíso, Valparaíso, Chile
[d] Sorbonne Université, INSERM, CNRS, Laboratoire d'Imagerie Biomédicale, LIB, F-75006 Paris, France
[e] Department of Imaging Physics, Delft University of Technology, Delft, the Netherlands

ARTICLE INFO

Keywords:
Ultrasonic imaging
Doppler measurement
Oil-in-water emulsion
Particle tracking
Velocimetry
Blood mimicking fluids

ABSTRACT

Blood-mimicking fluids (BMFs) play a critical role in ultrasonic imaging and Doppler flow studies by replicating the physical and acoustic properties of blood. This study introduces a novel soybean oil-in-water emulsion as a BMF with particle size akin to red blood cells. Using a millifluidic device, we cross-validated flow profiles through both Doppler velocimetry and optical particle tracking, demonstrating compatibility with theoretical Poiseuille flow models. The millifluidic chip, fabricated via stereolithography, provided an optimized platform for dual optical and ultrasonic assessments. Results showed strong agreement between the two methods across a range of flow rates, affirming the suitability of the emulsion for velocimetry applications. Furthermore, the acoustic properties of soybean oil droplets support their potential as an echogenic and stable alternative to conventional BMFs.

1. Introduction

Blood mimicking fluids (BMFs) are synthetic substances designed to simulate the acoustic and physical properties of human blood for use in ultrasonic imaging and Doppler flow studies [1]. These fluids typically consist of a water-glycerol base with suspended particles, aiming to replicate blood's density, viscosity, and acoustic characteristics [2]. While BMFs offer significant advantages over using actual blood, such as reduced biohazard risks and improved stability, they face challenges in accurately replicating blood's complex behavior [3]. Traditional BMFs often use solid particles like nylon or polystyrene at low concentration to mimic blood ultrasonic properties [1]. However, these particles cannot be used at concentrations as high as red blood cells in blood, and their non-deformable nature makes it difficult to study flow in small capillaries [1]. These limitations highlight the need for new BMF formulations that can better address these constraints.

Oil-in-water emulsions present a promising alternative, as they can be engineered with a narrow size distribution closely matching that of red blood cells [4]. Various vegetable oils can be used to create these emulsions, potentially offering a new class of BMFs with improved properties [5]. In this paper, we demonstrate that soybean oil-in-water emulsions can serve as effective BMFs. We provide a cross-calibration of the flow profile in a 3D printed millifluidic channel using both light microscopy and Doppler measurement techniques. Furthermore, we show that these measurements can be used for non-destructive determination of millifluidic channel dimensions by analyzing flow velocity as a function of the suspension's flow rate.

2. Materials and methods

2.1. Materials

Pluronic F-68 (Poloxamer 188, CAS no. 9003-11-6), Tween 20 (polyethylene glycol sorbitan monolaurate, CAS no. 9005-64-5) and soybean oil (CAS no. 8001-22-7) were purchased from Sigma-Aldrich (Saint Quentin Fallavier, France). Nano Clear resin (FunToDo) was purchased from Atome3D (Pechbonnieu, France). Propanol-2 (CAS no. 67–63-0) was purchased from VWR Chemicals (Rosny-sous-Bois,

* Corresponding authors at: Laboratoire P.A.S.T.E.U.R., Département de Chimie, École Normale Supérieure, PSL Research University, Sorbonne Université, CNRS, 75005 Paris, France.
E-mail addresses: jean-gabriel.minonzio@uv.cl (J.-G. Minonzio), jacques.fattaccioli@ens.psl.eu (J. Fattaccioli).

https://doi.org/10.1016/j.mne.2025.100298
Received 30 January 2025; Received in revised form 8 April 2025; Accepted 1 May 2025
Available online 8 May 2025

France). Ultrapure water (Millipore, 18.2 MΩ.cm) was used for all experiments. All reagents and materials were used as purchased, without any further purification.

2.2. Droplets fabrication

Droplets were fabricated using a Shirasu Porous Glass membrane emulsification apparatus (SPG Technology *Co*., Ltd., Japan), with a porous membrane. This membrane is immersed in an aqueous solution containing 15 % *w*/w of Pluronic F68 block copolymer. A pressure is applied by compressed air to the dispersed lipophilic phase, which is contained in a connected reservoir. Thus, this oil phase grows into droplets at the membrane pores (size = 2.1 μm). At a critical pressure, the droplets are extruded through the membrane and are stabilized in the continuous phase. The emulsion is continuously stirred throughout the process. The diameter dispersion was determined over 100 droplets and fitted with a Gaussian curve. The emulsion is stored in the dark at a constant temperature of 12 °C in a Peltier-cooled cabinet. Prior to the experiments, the emulsion is diluted into either a 1 % or a 10 % particle volume fraction in the Pluronic F68 aqueous solution, for optical and ultrasonic measurements respectively.

2.3. Design and fabrication of the Millifluidic device

The millifluidic chip was designed using the CAD software Tinkercad. It features a closed channel positioned 1 mm from both the top and bottom surfaces, with a square cross-section of 2 × 2 mm^2. Inlet and outlet ports were incorporated on either side of the channel for connectivity. The STL chip design was sliced using Chitubox software. Fabrication was performed with an Elegoo Mars 2 Pro SLA 3D printer and a transparent FunToDo Nanoclear resin to obtain an optically transparent chip. A 26x76mm microscopy glass slide was affixed to the build platform with double-sided tape to ensure a smooth surface at the bottom of the chip. Printing parameters were adjusted to enhance adhesion between the resin and the glass slide. Particularly, exposure time for bottom layers was increased with respect to the default setting values. Both lifting speed and the delay at the platform's maximal height were increased with respect to the default setting values to ensure the clearest channel with the minimal amount of residual and uncured resin.

The printing process was paused after the last channel layers were completed, and 2-propanol was flushed through the channel to remove any residual resin. Printing was then resumed to complete the chip. The final object was detached from the glass slide, cleaned in a 2-propanol bath for 6 min, dried, and subjected to a final light curing process with the Elegoo Mercury Plus during 8 min.

2.4. Millifluidic experiment

The inlet and outlet of the millifluidic chip were equipped with Luer locks and blunt-end Luer lock syringe needles. Plastic tubing (inner diameter: 0.02 in., outer diameter: 1/16″, Tygon, Saint-Gobain PPL Corp.) was attached to the opposite end of each needle. The inlet tubing was connected to a 5 mL plastic syringe (Terumo, Japan) via an additional needle. The syringe, prefilled with a diluted droplet suspension, was linked through plastic tubing. All connections—including those at the inlet, outlet, and syringe—were sealed with Teflon tape to prevent leakage. Flow rates, ranging from 60 to 360 $\mu L.min^{-1}$, were controlled by a syringe pump (NE-4000, New Era Pump Systems, USA), which drove the droplets through the chip. The droplets were collected at the outlet in a glass bottle for reuse.

2.5. Flow vector velocity mapping

A phased-array transducer (P4–1, ATL Philips, Bothell, WA, USA) operating at a center frequency of 2.5 MHz (96 elements, 0.295 mm pitch, the aperture of the probe in the elevation direction was 14 mm) was connected to a fully programmable ultrasound scanner (Vantage 256, Verasonics, Kirkland, WA, USA). A sequence of 15 tilted plane waves (steering angles ranging from −18 to +18 degrees) was used to make US images at a frame rate (or temporal sampling rate of the flow) of 440 Hz during 4.5 s. A coupling gel was used between the probe and the millifluidic chip. Images were reconstructed with a F-number of 1.3, therefore the spatial lateral resolution in the image was close to 1.1 mm (in the millifluidic phantom material). The temporal duration of the ultrasound pulse determines the spatial axial resolution (i.e., in the resolution along the depth direction), which was close to 0.7 mm (in the millifluidic phantom material). The height of the piezoelectric elements in the phased-array transducer determines the spatial elevational resolution (image thickness), which is close to 14 mm.

In order to extract the echo signal of the moving particles, we applied a temporal band-pass filter (4th order butterworth with cutoff frequencies 0.5 Hz and 6 Hz). The flow velocity and direction were estimated and mapped using a multi-angle plane wave imaging method [6] with refraction correction similar to [7] initially developed for intracortical bone imaging. The scanned region is described with two layers: the coupling gel and the phantom material. Applying an autofocus method as described in [8,9], we estimated the compressional wave speed in the coupling gel (1620 $m.s^{-1}$) and the millifluidic phantom material (2200 $m.s^{-1}$). The segmentation of the interface between the coupling gel and the phantom enabled the correction of wave refraction during image reconstruction and flow quantification. In order to enhance the signal-to-noise ratio and the spatial specificity of the signal received from the flowing particles, 3 synthetically focused transmit angles (−15 degrees, 0 degree and + 15 degrees) were generated from the 15 plane wave transmit angles. Next, the ultrasound images were reconstructed with 4 receive angles (−20 degrees, −10 degrees, +10 degrees and + 20 degrees) and wave refraction was taken into account. Therefore 12 combinations of transmit and receive angles were used to calculate the least-square estimate and map the velocity vector in the channel.

2.6. Optical measurements

Brightfield microscopy images used to monitor droplet flow (1 % oil volume fraction) were captured using a Leica DM IL LED inverted microscope equipped with 10× (N.A. = 0.22) and 20× (N.A. = 0.3) objectives. For droplet size measurements, images were acquired with a 40× objective (3-N-Achroplan, Zeiss, N.A. = 0.65). All images were recorded with an IDS camera (U3-3080CP-C-HQ, Rev.2.2), operated via the IDS Peak Cockpit software (version 1.5.0.0), which facilitated data retrieval, including corresponding timestamps for velocity measurements.

Images of the printed millifluidic device were captured using a motorized 2D/3D microscope (MRCL700 3D Imager Pro, MicroQubic AG, Switzerland), integrated with its proprietary camera.

2.7. Surface analysis

The surface imaging was realized with the MicroCubic MRCL700 3D Imager Pro (MicroQubic AG, Switzerland). The surface profilometry was executed with the Dektak 6 M Stylus Profiler (Veeco, Plainview, NY, USA), with a 12.5 μm radius stylus.

2.8. Image analysis

Image analysis was performed with ImageJ/Fiji (version v1.54h) [10] and data analyses were performed with Matlab (MathWorks, Natick, MA, USA) software (R2022b version).

3. Results and discussion

We prepared a blood-mimicking fluid using a soybean oil-in-water

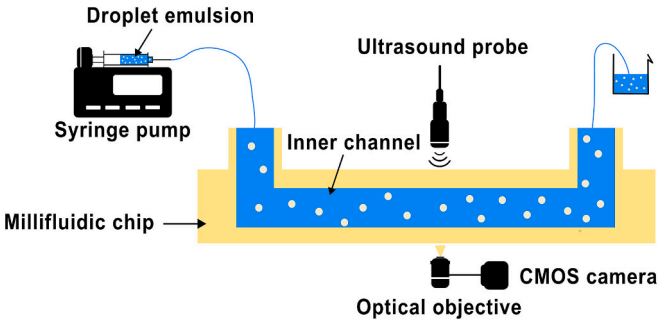

Fig. 1. Schematic representation of the experimental setup for droplets velocity tracking through two techniques: optical tracking and ultrasound probing. Droplets are introduced, at a controlled flow rate, by a syringe pump through the millifluidic chip in which the velocities are measured.

emulsion suspension. While maintaining a continuous controlled flow rate of the suspension in a millifluidic channel, we measured the flow rate of the oil droplets both by optical particle trapping and Doppler velocimetry, as sketched in Fig. 1. Experimental details are given in the Methods section.

3.1. Formulation of the blood-mimicking fluid

The particle suspension is an emulsion of soybean oil-in-water droplets fabricated using a membrane-emulsification apparatus, as sketched in Fig. 2A, B and detailed in the Methods section. This technique consists in forcing an oil phase, here soybean oil, through a porous membrane into an aqueous phase containing surfactants, resulting in a size-controlled emulsion [11].

The droplets are stabilized in an aqueous continuous phase of Pluronic F68 15 % *w*/w (Fig. 2C). In order to mimic the size of red blood cells, whose diameter is between 6 and 8 µm [12], we chose to work with a 2.1-µm-pore-size membrane, resulting in 8.8 ± 0.6 µm droplets, giving a variation coefficient of ca. 7 % (Fig. 2D). Prior to the experiments, the initial emulsion fabrication batch is diluted in Pluronic F68 aqueous solution at two different concentrations for the two different tracking strategies.

First, a droplet suspension with a volume fraction of 1 % is prepared in order to track particles individually by optical method. Indeed, soybean oil has an optical refractive index of 1.48 [13], much higher than the refractive index of the aqueous continuous phase ($n = 1.33$). This optical property gives an excellent optical contrast on the pictures of the droplets, hence easing the tracking if the droplet concentration is low

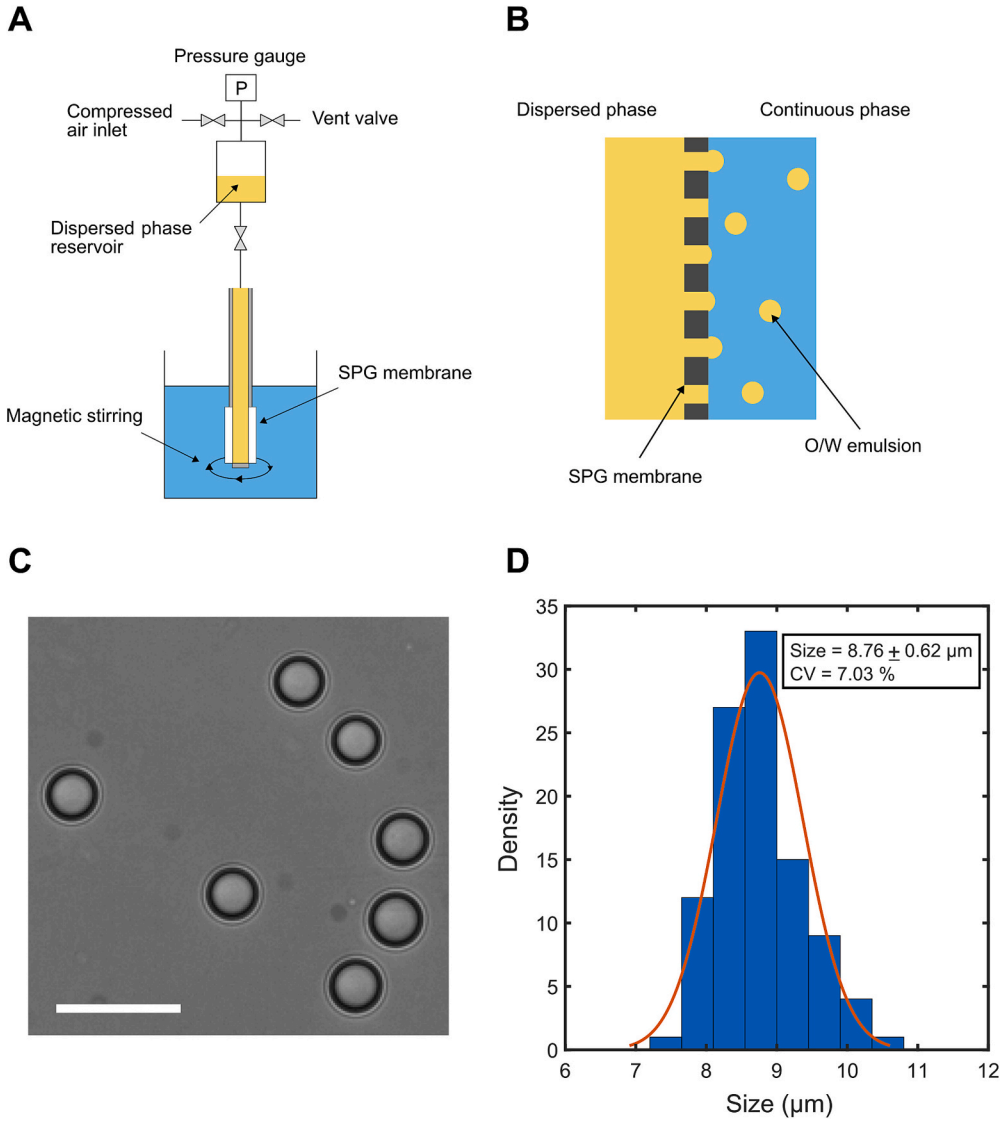

Fig. 2. (A) Principle of the emulsification through a SPG membrane. (B) Porous membrane scheme for an oil-in-water emulsion. Scale bar: 20 µm (C) Brightfield image of soybean oil droplets used as blood-mimicking fluid for flow tracking. (D) Size distribution histogram of the oil-in-water emulsion.

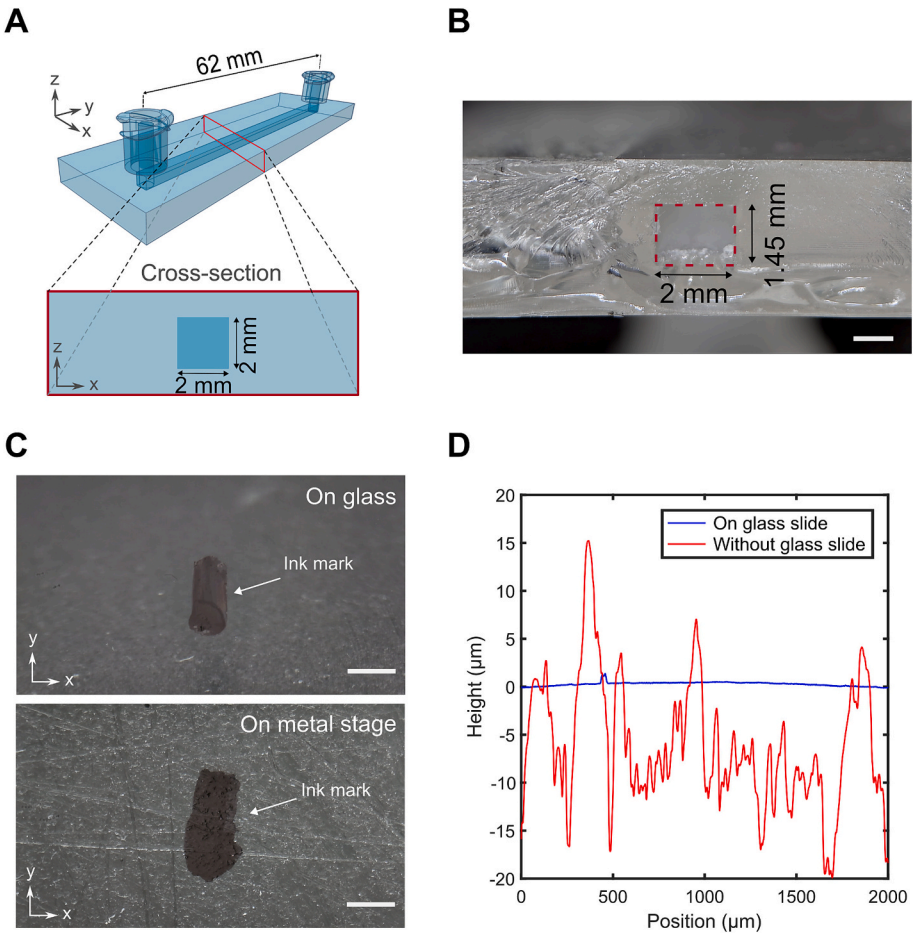

Fig. 3. (A) CAD representation of the printed millifluidic device with the cross sectional representation. (B) Cross sectional image of the printed device, with the resulting rectangular channel within the dotted rectangle. Scale bar: 2 mm. (C) Surfaces imaging of the device's bottom with and without a glass slide as the build plate. Scale bar: 1 mm. (D) Corresponding surface profilometry of the two printing techniques presented in (C).

enough to segment individual droplets.

Conversely, the acoustic velocity in vegetable oils, including soybean oil, in the ultrasonic range of 2 to 3 MHz is approximately 1460–1470 m.s^{-1} at room temperature [14]. This value is very close to the acoustic velocity in water, which is around 1480 m.s^{-1} in the same frequency range. Likewise, the mass density of soybean oil, ranging from 0.919 to 0.925 g.cm^{-3}, is close to the water value (1 g.cm^{-3}). Thus, the receptive acoustic impedances for soybean oil and water are about 1.34–1.36 and 1.46–1.47 MRayl. These small velocity and density differences imply that the impedance contrast, i.e., about 0.1 MRayl, and therefore the amplitude of the backscattered signal are low, with a reflection coefficient less than 5 % in amplitude. Note that this small impedance difference with respect to water is comparable with differences observed between soft tissues, typically about 1,58 MRayl [15] and blood cells, about 1.65–1.75 MRayl [16]. Note that conventional commercial BMFs use particles of polymer, such as nylon or polystyrene [17], with typical impedances ranging from 2.4 to 3.2 MRayl, i.e., implying a higher and less realistic impedance contrast. Note that a more realistic BMF has been recently proposed [3]. Based on water-soluble silicone oil, the impedance is about 1.65 ± 1.2 MRayl, close to the actual blood values. In clinical practice, the individual small acoustic signal of each blood cell, due both small contrast impedance and size, is compensated by a large concentration, normally about 4 to 50 % [18]. Similarly our ultrasonic strategy considered a higher volume fraction to amplify the signals received from the sample. Therefore, we worked at a concentration of 10 % in volume for the Doppler velocimetry.

3.2. *Millifluidic device design and fabrication*

To perform the dual optical and ultrasonic flow velocity measurements, we designed a simple millifluidic chip consisting of a straight channel with a 2 × 2 mm square cross-section, using a CAD software as shown on Fig. 3A. This model was manufactured by stereolithography (SLA), with a transparent resin. To ensure reliable velocimetry measurements, dimensional evaluation was required. When comparing the channel's designed cross-sectional dimensions with those of an actual printed device, a discrepancy is observed, particularly in the height, which results in a 2 × 1.45 mm^2 rectangular cross-section instead of the intended square one, as shown on Fig. 3B.

An optimization of the device's roughness during the printing process is required in order to improve the emulsion's imaging. Therefore the chip was printed using a glass slide as a building support using a custom-made setup (see Methods for details) to obtain a smooth bottom surface. The smoothness improvement is assessed by comparing devices printed on different supports: either on the conventional metallic building platform or on a glass slide. Fig. 3C illustrates the difference in surface roughness between the two printing methods. Visually, the side printed on the metallic building platform exhibits a more irregular surface compared to the one obtained on glass, which appears more homogeneous.

This observation is confirmed by the topography analysis performed using profilometry (see Fig. 3D). The surface profile for the added glass slide is relatively smooth, with minimal variations around the mean height. In contrast, the typical platform shows significantly higher

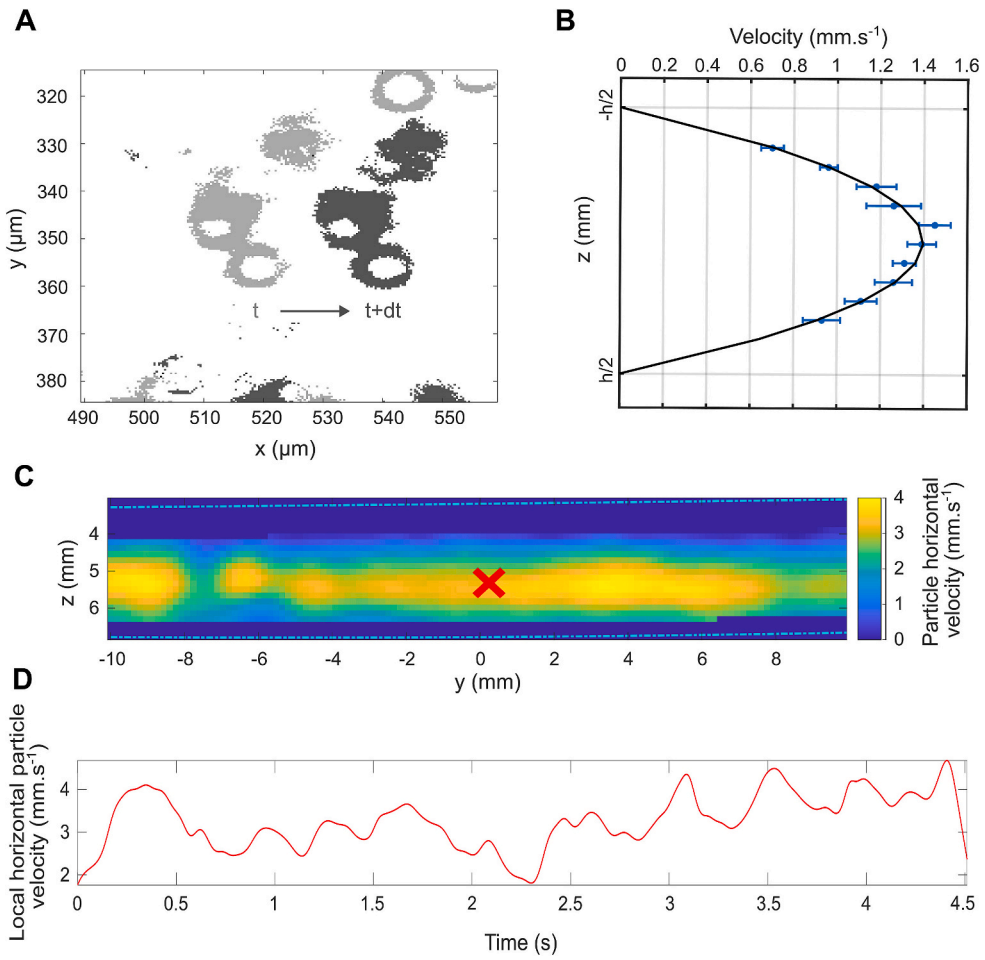

Fig. 4. (A) Two consecutives images superposed representing a droplet displacement in the millifluidic chip used for optical tracking. This experiment was taken with a flow rate of 60 µL.min^{-1}, at a particle concentration of 1 vol%. (B) Velocity profile of droplets along the z-axis within the channel. The black line corresponds to the parabolic extrapolation coming from the optical measures. The resulting maximal velocity of 1.4 mm.s^{-1} is deduced from the extrapolation. This profile was analyzed for a flow rate of 120 µL.min^{-1}. (C) Mapping of the flow velocity within the channel estimate with ultrasound flow vector velocimetry at a flow rate of 360 µL.min^{-1}. The red cross represents the local point where the velocity is measured as a function of time in (D). (For interpretation of the references to colour in this figure legend, the reader is referred to the web version of this article.)

roughness, characterized by pronounced fluctuations in the surface profile.

3.3. Optical and ultrasonic dual velocity measurements

To vary the flow rates within the 3D-printed microchannel, the continuous flow was adjusted across a range of 60 to 360 µL.min^{-1} with a syringe pump, simulating the lower values commonly observed in the bloodstream [7,19].

For the optical characterization of the flow, the microscope objective is moved from the bottom to the top of the channel to capture the complete variation of the axial velocity profile. The channel's bottom is identified by observing adsorbed impurities on the inner wall of the bottom part of the channel. For each height increment of roughly 0.14 mm, an image sequence is recorded with a sufficiently high framerate (10–30 fps) to track the displacement of several particles within the observation field. For each time lapse recording, the instantaneous velocity V(z) of the particles is then measured by measuring their axial displacement Δx, measured by correlation analysis of pairs of successive images, over the sampling time frame Δt recorded by the camera (Fig. 4A). We can then reconstruct the parabolic velocity profile of the particles shown in Fig. 4B, typical of a Poiseuille flow. This is in accordance with the value of the Reynolds number of the system, which remains small with our flow rate conditions.

Two-dimensional vector ultrasonic velocimetry was performed. Because the flow channel is parallel to the transducer array surface, the particle velocity corresponds to the lateral component of the estimated velocity vector. Fig. 4C shows an example map of the particle velocity in the flow channel, as estimated with ultrasound imaging. As expected for a laminar flow, maximum flow velocity is observed in the middle of the channel (for a depth of approximately 5.5 mm). Fig. 4D displays the estimated flow velocity as a function of time, at the position depicted in Fig. 4C by the red cross. The lateral component of the estimated velocity vector was averaged temporally (over 4.5 s) and spatially within the flow channel in the ultrasound image.

3.4. Comparison of the two measurement techniques

The average velocity in the enclosed channel can be expressed [20] as a function of the volumetric flow rate Q along with the dimensional considerations, w being the width of the channel and h its height:

$$V_{average} = \frac{1}{wh} Q \tag{1}$$

Fig. 5 shows the average droplet velocity measured using optical microscopy (blue) and Doppler ultrasound (red). The two techniques demonstrate good agreement across the range of imposed flow rates. Assuming a channel width of w = 2 mm, which is consistent with

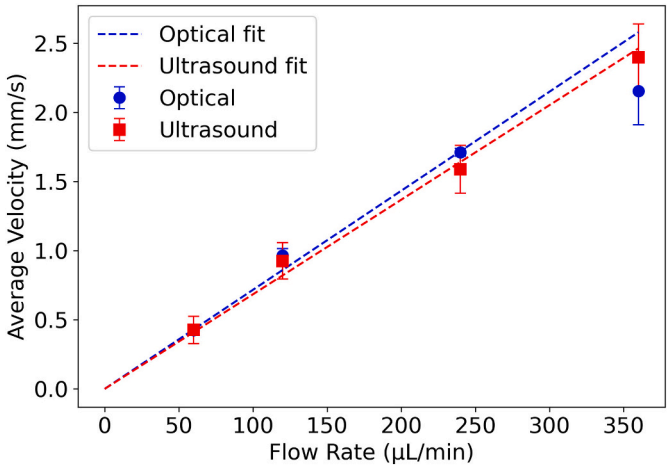

Fig. 5. Measurements of the average velocity of the droplet by optical microscopy (blue) and ultrasound probing (red) for various flow rates. The dotted lines represent the fitted average velocity obtained taking $w = 2$ mm as the constant parameter and. The fitted h is respectively equal to 1.22 +/− 0.018 mm and 1.28 +/− 0.076 mm for the optical and the Doppler measurements. (For interpretation of the references to colour in this figure legend, the reader is referred to the web version of this article.)

measurements along the entire millifluidic chip, fitting the experimental data yields channel height estimates of h = 1.22 ± 0.018 mm for optical measurements and h = 1.28 ± 0.076 mm for Doppler measurements.

To assess the actual channel height, we performed direct measurements at two different locations along the chip, obtaining values of h = 1.44 mm and h = 1.56 mm. These results highlight that the channel height is not perfectly uniform along its length.

While the width of the 3D-printed channels closely matches the CAD design, the resin's viscosity makes it more challenging to maintain a consistent height throughout the channel. As a result, discrepancies between the theoretical height (from the CAD model) and the actual printed height are expected and must be considered when evaluating deviations from the model.

Recent advances in the formulation of resins for 3D printing of enclosed milli- and microfluidic structures [21] offer promising solutions to this limitation, especially when higher dimensional precision and uniformity are required.

It is worth noting that different oil volume fractions were utilized for optical (1 %) and Doppler ultrasound (10 %) measurements, due to practical experimental constraints. Optical tracking at higher droplet concentrations became challenging because of image segmentation limitations caused by channel surface roughness. Conversely, Doppler measurements required a higher droplet concentration to compensate for the inherently low echogenicity of soybean oil droplets and to ensure a sufficient ultrasound signal-to-noise ratio. To assess whether this difference might impact comparability between measurement methods, we estimated the emulsion viscosity at these two volume fractions using the relation from Nawab and Mason [22]. The relatively small viscosity variation (less than 30 %) between 1 % and 10 % concentrations indicates that the difference in concentration has a negligible effect on the flow velocity profiles measured, thus validating the comparability of the results obtained by both measurement techniques.

Compared to traditional blood-mimicking fluid (BMF) formulations, our soybean oil-in-water emulsion offers several significant advantages. Conventional BMFs typically employ glycerol-water solutions with rigid polymer microparticles, such as nylon or polystyrene [3]. Although these microparticles have standardized sizes, their rigid nature prevents realistic emulation of red blood cell deformability, particularly in narrow or complex flow geometries. Moreover, rigid microparticles often face concentration limitations due to sedimentation and aggregation, compromising echogenicity and rheological realism. Additionally, unlike the predominantly Newtonian behavior of glycerol-based fluids, soybean oil-in-water emulsions exhibit shear-thinning rheology [23] closely resembling blood's complex flow characteristics.

Another critical advantage is the emulsion's echogenicity. Edible oils such as soybean oil have established acoustic properties suitable for ultrasound-based measurements, including appropriate speed-of-sound characteristics, as shown by our experiments. Although soybean oil droplets have not been extensively explored as ultrasound contrast agents, our results indicate adequate echogenicity for Doppler measurements. Despite a lower acoustic velocity (~1460–1470 $m \cdot s^{-1}$, similar to water) compared to rigid polymer-based BMFs, the shear-thinning behavior of soybean oil emulsions better approximates blood rheology. This property is particularly advantageous, as it potentially enables studies involving high concentrations of droplets, comparable to physiological conditions, while minimizing acoustic scattering and attenuation. Thus, this emulsion opens avenues for realistic flow measurements in microvascular or capillary-scale environments.

4. Conclusion

This study demonstrates the feasibility of using soybean oil-in-water emulsions as a blood-mimicking fluid for both optical and ultrasonic flow velocity measurements. The emulsion achieves a precise size distribution similar to red blood cells and exhibits excellent stability [24] and realistic echogenicity. Experimental results confirmed strong agreement between optical and Doppler measurements, validating the emulsion's performance in a 3D-printed millifluidic device. While certain physical properties, such as viscosity, were not optimized, the current formulation proved effective for velocimetry applications. The deformability [25] and acoustic properties of the droplets make them a promising candidate for future studies, particularly in mimicking complex blood behavior. Further research could expand their utility by tailoring rheological and acoustic properties to specific experimental needs.

Author contribution

EL: Investigation, Methodology, Validation, Visualization, Writing - original draft, Writing - reviewing and editing. WFC: Investigation. HU: Resources. AC: Resources. QG: Investigation, Writing - reviewing. GR: Conceptualization, Formal Analysis, Methodology, Supervision, Writing - original draft, Writing - reviewing and editing. JGM: Conceptualization, Methodology, Funding acquisition, Supervision, Visualization, Writing - original draft, Writing - reviewing and editing. JF: Conceptualization, Methodology, Funding acquisition, Supervision, Visualization, Writing - original draft, Writing - reviewing and editing.

Declaration of competing interest

The authors declare that they have no competing interests.

Data availability

Data will be made available on request.

Acknowledgments

This work was funded by the grant ANID ECOS-Sud 20,061 and the grant ANID / Fondecyt / Regulat 1,241,091. This work benefited from the technical contribution of the joint service unit CNRS UAR 3750. The authors would like to thank the engineers of this unit (and in particular Audric Jan and Elian Martin) for their advice during the development of the experiments. We thank Bastien Venzac (LAAS-CNRS) for additive manufacturing discussions. We thank Michel Cloître (3CM, ESPCI-PSL) for fruitful discussions about the viscosity of emulsion suspensions.

References

[1] K.V. Ramnarine, D.K. Nassiri, P.R. Hoskins, J. Lubbers, Validation of a new blood-mimicking fluid for use in Doppler flow test objects, Ultrasound Med. Biol. 24 (1998) 451–459, https://doi.org/10.1016/s0301-5629(97)00277-9.

[2] X. Zhou, P.R. Hoskins, Testing a new surfactant in a widely-used blood mimic for ultrasound flow imaging, Ultrasound 25 (2017) 239–244, https://doi.org/10.1177/1742271X17733299.

[3] A.A. Oglat, A review of blood-mimicking fluid properties using Doppler ultrasound applications, J. Med. Ultrasound. 30 (2022) 251–256, https://doi.org/10.4103/jmu.jmu_60_22.

[4] Y.N. Shariffa, T.B. Tan, U. Uthumporn, F. Abas, H. Mirhosseini, I.A. Nehdi, Y. H. Wang, C.P. Tan, Producing a lycopene nanodispersion: formulation development and the effects of high pressure homogenization, Food Res. Int. 101 (2017) 165–172, https://doi.org/10.1016/j.foodres.2017.09.005.

[5] S.M. Ali, B. Ali, Acoustics Impedance Studies in Some Commonly Used Edible Oils, 2014.

[6] B.Y.S. Yiu, A.C.H. Yu, Least-squares multi-angle Doppler estimators for plane-wave vector flow imaging, IEEE Trans. Ultrason. Ferroelectr. Freq. Control 63 (2016) 1733–1744, https://doi.org/10.1109/TUFFC.2016.2582514.

[7] S. Salles, J. Shepherd, H.J. Vos, G. Renaud, Revealing intraosseous blood flow in the human tibia with ultrasound, JBMR PLUS. 5 (2021) e10543, https://doi.org/10.1002/jbm4.10543.

[8] G. Renaud, P. Kruizinga, D. Cassereau, P. Laugier, In vivo ultrasound imaging of the bone cortex, Phys. Med. Biol. 63 (2018) 125010, https://doi.org/10.1088/1361-6560/aac784.

[9] R. Waasdorp, D. Maresca, G. Renaud, Assessing transducer parameters for accurate medium sound speed estimation and image reconstruction, IEEE Trans. Ultrason. Ferroelectr. Freq. Control 71 (2024) 1233–1243, https://doi.org/10.1109/TUFFC.2024.3445131.

[10] J. Schindelin, I. Arganda-Carreras, E. Frise, V. Kaynig, M. Longair, T. Pietzsch, S. Preibisch, C. Rueden, S. Saalfeld, B. Schmid, J.-Y. Tinevez, D.J. White, V. Hartenstein, K. Eliceiri, P. Tomancak, A. Cardona, Fiji: an open-source platform for biological-image analysis, Nat. Methods 9 (2012) 676–682, https://doi.org/10.1038/nmeth.2019.

[11] S.M. Joscelyne, G. Trägårdh, Membrane emulsification — a literature review, J. Memb. Sci. 169 (2000) 107–117, https://doi.org/10.1016/S0376-7388(99)00334-8.

[12] M. Diez-Silva, M. Dao, J. Han, C.-T. Lim, S. Suresh, Shape and biomechanical characteristics of human red blood cells in health and disease, MRS Bull. 35 (2010) 382–388, https://doi.org/10.1557/mrs2010.571.

[13] E.M. Abdo, O.E. Shaltout, H.M.M. Mansour, Natural antioxidants from agro-wastes enhanced the oxidative stability of soybean oil during deep-frying, LWT 173 (2023) 114321, https://doi.org/10.1016/j.lwt.2022.114321.

[14] C. Javanaud, R.R. Rahalkar, Velocity of sound in vegetable oils, Fett/Lipid 90 (1988) 73–75, https://doi.org/10.1002/lipi.19880900208.

[15] H. Azhari, Appendix a: Typical Acoustic Properties of Tissues, in: Basics of Biomedical Ultrasound for Engineers, John Wiley & Sons, Inc., Hoboken, NJ, USA, 2010, pp. 313–314, https://doi.org/10.1002/9780470561478.app1.

[16] P. Augustsson, J.T. Karlsen, H.-W. Su, H. Bruus, J. Voldman, Iso-acoustic focusing of cells for size-insensitive acousto-mechanical phenotyping, Nat. Commun. 7 (2016) 11556, https://doi.org/10.1038/ncomms11556.

[17] X. Zhou, D.A. Kenwright, S. Wang, J.A. Hossack, P.R. Hoskins, Fabrication of two flow phantoms for doppler ultrasound imaging, IEEE Trans. Ultrason. Ferroelectr. Freq. Control 64 (2017) 53–65, https://doi.org/10.1109/TUFFC.2016.2634919.

[18] B.J. Bain, Blood Cells: A Practical Guide, Wiley, 2022, https://doi.org/10.1002/9781119820307.

[19] V. Grand-Perret, J.-R. Jacquet, I. Leguerney, B. Benatsou, J.-M. Grégoire, G. Willoquet, A. Bouakaz, N. Lassau, S. Pitre-Champagnat, A novel microflow phantom dedicated to ultrasound microvascular measurements, Ultrason. Imaging 40 (2018) 325–338, https://doi.org/10.1177/0161734618783975.

[20] H.A. Stone, Introduction to fluid dynamics for microfluidic flows, in: H. Lee, R. M. Westervelt, D. Ham (Eds.), CMOS Biotechnology, Springer US, Boston, MA, 2007, pp. 5–30, https://doi.org/10.1007/978-0-387-68913-5_2.

[21] H. Shafique, V. Karamzadeh, G. Kim, M.L. Shen, Y. Morocz, A. Sohrabi-Kashani, D. Juncker, High-resolution low-cost LCD 3D printing for microfluidics and organ-on-a-chip devices, Lab Chip 24 (2024) 2774–2790, https://doi.org/10.1039/d3lc01125a.

[22] M.A. Nawab, S.G. Mason, The viscosity of dilute emulsions, Trans. Faraday Soc. 54 (1958) 1712, https://doi.org/10.1039/tf9585401712.

[23] H.A. Barnes, Rheology of emulsions — a review, Colloids Surf. A Physicochem. Eng. Asp. 91 (1994) 89–95, https://doi.org/10.1016/0927-7757(93)02719-U.

[24] K.C. Powell, R. Damitz, A. Chauhan, Relating emulsion stability to interfacial properties for pharmaceutical emulsions stabilized by Pluronic F68 surfactant, Int. J. Pharm. 521 (2017) 8–18, https://doi.org/10.1016/j.ijpharm.2017.01.058.

[25] D. Molino, S. Quignard, C. Gruget, F. Pincet, Y. Chen, M. Piel, J. Fattaccioli, On-Chip quantitative measurement of mechanical stresses during cell migration with emulsion droplets, Sci. Rep. 6 (2016) 29113, https://doi.org/10.1038/srep29113.